

# Quenched chirality in RbNiCl<sub>3</sub>

Maikel C. Rheinstädter\* and Mechthild Enderle

*Institut Laue-Langevin, 6 rue Jules Horowitz, BP 156, 38042 Grenoble Cedex 9, France and  
Technische Physik, Universität des Saarlandes, PSF 1551150, 66041 Saarbrücken, Germany*

Garry McIntyre

*Institut Laue-Langevin, 6 rue Jules Horowitz, BP 156, 38042 Grenoble Cedex 9, France*

(Dated: May 23, 2019)

The critical behaviour of stacked-triangular antiferromagnets has been intensely studied since Kawamura predicted new universality classes for triangular and helical antiferromagnets. The new universality classes are linked to an additional discrete degree of freedom, chirality, which is not present on rectangular lattices, nor in ferromagnets. However, the theoretical as well as experimental situation is discussed controversially, and generic non-universality has been proposed as an alternative scenario. Here we present a careful investigation of the zero-field critical behaviour of RbNiCl<sub>3</sub>, a stacked-triangular Heisenberg antiferromagnet with very small Ising anisotropy. From linear birefringence experiments we determine the specific heat exponent  $\alpha$  as well as the critical amplitude ratio  $A^+/A^-$ . Our high-resolution measurements point to a single second order phase transition with standard Heisenberg critical behaviour, contrary to all theoretical predictions. From a supplementary neutron diffraction study we can exclude a structural phase transition at  $T_N$ . We discuss our results and the outcome of a supplementary neutron diffraction experiment in the context of other available experimental results on RbNiCl<sub>3</sub> and related compounds. We arrive at a simple intuitive explanation which may be relevant for other discrepancies observed in the critical behaviour of stacked-triangular antiferromagnets. In RbNiCl<sub>3</sub> the ordering of the chirality is therefore suppressed by strong spin fluctuations. This yields to a different phase diagram, as compared to e.g. CsNiCl<sub>3</sub>, where the Ising anisotropy prevents these fluctuations.

PACS numbers: 75.25.+z, 75.50.Ee, 75.40.Gb, 75.10.Jm,

Keywords: spin systems; spin fluctuations; rubidium compounds

On a hexagonal lattice, an antiferromagnet can never entirely satisfy its interactions, they will be at least partially frustrated. A stacked set of triangular planes will nevertheless develop long-range order for any finite inter-plane interaction. In the perfectly isotropic case (Heisenberg antiferromagnet), neighboring spins on a triangle compromise the antiferromagnetic interaction by including 120 °, along the hexagonal axis the spins will be collinear. The magnetic structure is then defined by two continuous degrees of freedom (the polar and azimuthal angle of one chosen spin) and one additional discrete degree of freedom, the chirality, the sense of rotation of the spin direction on a chosen triangle. This chirality vanishes in collinear structures, on rectangular lattices and in ferromagnets. It is still present for easy-plane antiferromagnets, and in the spin-flop phases of antiferromagnets with a small Ising-anisotropy. A large family of hexagonal compounds with a chiral degree of freedom can be described by the Hamiltonian

$$H = J \sum_{i,j} \text{intra chain} \mathbf{S}_i \cdot \mathbf{S}_j + J' \sum_{i,k} \text{inter chain} \mathbf{S}_i \cdot \mathbf{S}_k - D \sum_i (S_i^z)^2. \quad (1)$$

Here,  $J > 0$  denotes the antiferromagnetic exchange interaction between nearest neighbours along the symmetry axis,  $J' > 0$  the antiferromagnetic interaction between nearest neighbours on a triangle. The single ion anisotropy constant  $D$  favors an easy-axis ( $D > 0$ ) or

plane ( $D < 0$ ). Kawamura<sup>1</sup> predicted that the chiral degree of freedom provokes not only a different topology of the field-temperature phase diagrams, but also new types of universal critical behaviour, the  $n = 2$  chiral and the  $n = 3$  chiral universality class. This prediction is discussed controversially, and arguments have been given for quite different scenarios, as e.g. generic non-universal behavior<sup>2</sup>. Table I lists Kawamura's predictions for the critical exponents  $\alpha$ ,  $\beta$ ,  $\gamma$  and  $\delta$  and the ratio  $A^+/A^-$  for antiferromagnets on rectangular and triangular lattices as a survey.

ABX<sub>3</sub> compounds with easy-axis anisotropy, as CsNiCl<sub>3</sub>, RbNiCl<sub>3</sub>, CsMnI<sub>3</sub> and CsNiBr<sub>3</sub> are well described by the Hamiltonian in Eq. (1) and have developed model systems for low dimensional fluctuations and ordering, see e.g. [3] for a recent review. These compounds show quasi one-dimensional (1D) magnetic behavior, because the intrachain interaction  $J$  is much larger than the interchain interaction  $J'$ , typically  $J'/J \approx 10^{-2}$ . One-dimensional short-range antiferromagnetic order within the 1D spin chains develops below about 40 K. At lower temperatures there is a phase transition into a three-dimensionally (3D) magnetically ordered structure. Without an external field, Heisenberg antiferromagnets with an Ising anisotropy on a triangular lattice undergo two successive phase transitions, where ordering of the spin components parallel and perpendicular to the hexagonal *c*-axis occurs at  $T_{N1}$  and  $T_{N2}$  ( $< T_{N1}$ ), respectively. Below  $T_{N2}$ , the spins form a 120 ° structure in the *ac*

		$\alpha$	$\beta$	$\gamma$	$\nu$	$A^+/A^-$
$\square$	Ising	0.1098(29)	0.325(1)	1.2402(9)	0.6300(8)	0.55
	XY	-0.0080(32)	0.346(1)	1.3160(12)	0.6693(10)	0.99
	Heisenberg	-0.1160(36)	0.3647(12)	1.3866(12)	0.7054(11)	1.36
$\triangle$	n=2 chiral	0.34(6)	0.253(10)	1.13(5)	0.54(2)	0.36(2)
	n=3 chiral	0.24(8)	0.30(2)	1.17(7)	0.59(2)	0.54(2)

TABLE I: Critical exponents for antiferromagnets on square and triangular lattices after Kawamura, see [3,4,5] and references therein.

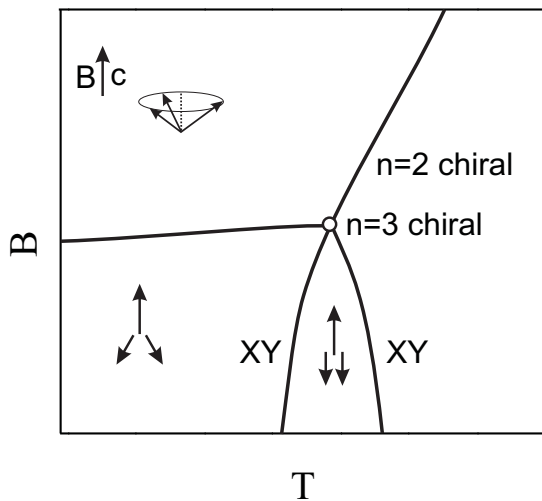


FIG. 1: Predicted phase diagram for  $ABX_3$  with easy-axis anisotropy. In zero magnetic field, two successive phase transitions are expected, connected with ordering of the spin components parallel and perpendicular to the hexagonal  $c$ -axis at  $T_{N1}$  and  $T_{N2}$  ( $< T_{N1}$ ), respectively. Both transitions should show XY critical behavior.

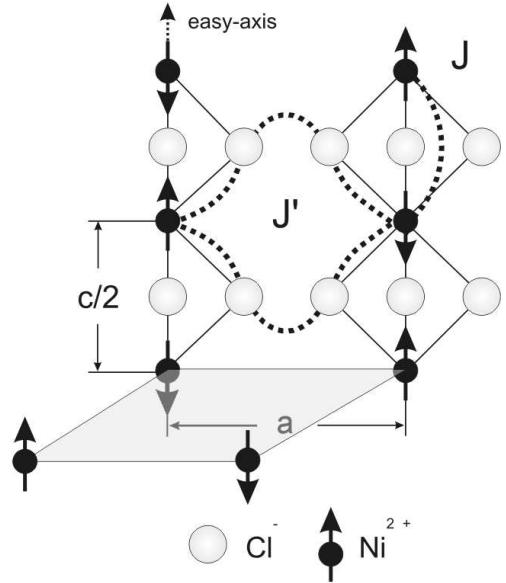


FIG. 2: In  $RbNiCl_3$  magnetic exchange  $J$  along the easy-axis is two orders of magnitude larger than exchange in the basal plane  $J'$ , which involves two  $Cl^-$ -ions (as compared to one along  $c$ ).

## I. RBNICL<sub>3</sub>

plane. The predicted B-T phase diagram is schematically shown in Fig. 1. The two zero-field phase transitions should show 3D XY-critical behavior<sup>1</sup>. On a rectangular lattice, there is just one transition with Ising-type critical behavior<sup>3,4,5</sup>.

In order to clarify the number of phase transitions in  $RbNiCl_3$ , and their criticality, we performed linear magnetic birefringence (LMB) experiments with a high temperature resolution to measure the critical exponent  $\alpha$  and the amplitude ratio  $A^+/A^-$ . The paper is organized as follows: The properties of  $RbNiCl_3$  are discussed in Sect. I. Experimental details of the birefringence set-up are presented in Sect. II, the LMB results and the outcome of a supplementary neutron diffraction study are shown and discussed in Sect. III. The anomalous behavior of  $RbNiCl_3$  as compared to other members of the above mentioned  $ABX_3$  family, is discussed in the discussion in Sect. IV.

$RbNiCl_3$  is a quasi 1D  $S=1$  Heisenberg antiferromagnet with a weak Ising anisotropy on a triangular lattice (hexagonal space group  $P6_3/mmc$ ). As in other members of the  $ABX_3$  family,  $CsNiCl_3$ ,  $CsMnI_3$ ,  $CsNiBr_3$  and  $RbNiBr_3$ , the magnetic  $Ni^{2+}$ -ions form strongly coupled chains along the crystallographic  $c$ -axis. The chains are characterized by an intrachain exchange parameter  $J$ , which is much larger than the interchain exchange parameter  $J'$  because magnetic exchange in the basal plane is mediated via two X-ions compared to only one along  $c$ , as pictured in Fig. 2.  $J'/J = 0.38K/23.8K = 1.6 \cdot 10^{-2}$  in  $RbNiCl_3$ <sup>6</sup>. The magnetic behavior therefore is quasi 1D. At  $T_N \simeq 11$  K, there is a phase transition into a 3D magnetically ordered structure.

Magnetic ordering in  $RbNiCl_3$  can be discussed in the context of other members of the  $ABX_3$  family. In e.g.  $CsNiCl_3$ , two successive phase transitions are found in neutron scattering, magnetic birefringence and specific heat capacity experiments and display 3D XY-critical be-

Technique	Ref.	$T_N$ (K)	$\alpha$	$\beta$
neutron diffraction	[7]	11.15		$\beta = 0.30 \pm 0.01$
	[8]	11.11,11.25		$\beta_{\parallel,\perp} = 0.27 \pm 0.01, 0.28 \pm 0.01$
LMB	[9]	11	0.06 $\pm$ 0.04	
	[10]	11.3		
	[11]	11		
NMR	[12]	11.18,11.36 (?)		
susceptibility, torque	[13,14]	11.38		
magnetization, susceptibility	[15]	11		
thermal expansion	[16]	11.2		
specific heat capacity	[16,17]	11.0		

TABLE II: Reported results for the zero-field phase transition in  $\text{RbNiCl}_3$ . Values for the relation  $A^+/A^-$  are not given in the references.

havior with the corresponding critical exponents<sup>3,18</sup>, as predicted by Kawamura. For  $\text{RbNiCl}_3$ , with most experimental techniques just one transition is observed. The criticality of this transition is not clear: Different methods obtained disagreeing values of the critical exponents and accordingly different universality classes have been proposed for the transition. None of the experimentally determined values agrees with the prediction for the 3D XY class. Table II summarizes experimental techniques and the values determined for  $T_N$ ,  $\alpha$  and  $\beta$ , as found in literature. Apart from a neutron scattering study by Oohara *et al.*<sup>10</sup>, all measuring techniques report only one phase transition. The temperature resolution in all experiments was better than 0.02 K, considerably smaller than 0.15 K, claimed as the distance between  $T_{N1}$  and  $T_{N2}$  in the neutron scattering study. The anomalies in all techniques appear very sharp while the overlap of two close lying divergences would lead to a rounded and broad anomaly. Furthermore, the measured critical exponents do not coincide with the predicted 3D XY-critical behavior. If the two transitions would fall together at the same temperature, the transition from the paramagnetic directly into the chiral ordered state should show  $n=3$  chiral exponents, against the experimental evidence.

$\text{RbNiCl}_3$  has a very small Ising anisotropy  $D$ , as compared to other members of the  $\text{ABX}_3$  family. We argue that the pronounced Heisenberg character plays the key role for the understanding of phase transitions and criticality in  $\text{RbNiCl}_3$ . In the next section, we present and discuss the results of our high resolution LMB experiments.

## II. EXPERIMENTAL

The linear birefringence  $n_{ac} = n_c - n_a$  has been measured using a Sénarmont set-up<sup>19,20</sup> with a He-Ne laser at  $\lambda=632.8$  nm. Before and behind the sample, apertures with a diameter of 0.3 mm were installed. The sensitivity of the Sénarmont set-up was increased by modulating the incoming polarisation with 50 kHz and lock-in detection of the intensity. Single crystals of  $\text{RbNiCl}_3$  were

grown by the Bridgeman method. The slightly hygroscopic samples were prepared by cleaving in a glovebox under He-atmosphere. The natural cleavage planes contain the  $c$ -axis, and correspond probably to  $\{10\bar{1}0\}$ . The typical sample size was  $4 \times 4 \times 1.5$  mm<sup>3</sup>. The cleft samples were used without further polishing and were mounted stress-free in an optical <sup>4</sup>He continuous flow cryostat with a temperature stability of 0.001 K. The sample temperature was measured with a Cernox semiconductor thermometer in lock-in technique with a relative accuracy of 0.001 K.

Under certain conditions, the derivative  $dn_{ac}/dT$  is proportional to the magnetic part of the specific heat capacity, see e.g. [21] and references therein. This relation is in particular valid close to the phase transitions of the antiferromagnetic triangular  $\text{ABX}_3$  compounds with and without easy-axis anisotropy, as  $\text{CsNiCl}_3$  and  $\text{RbNiCl}_3$ . In the temperature range of the phase transition in  $\text{RbNiCl}_3$  at  $T_N \approx 11$  K, the specific heat capacity is already dominated by contributions of the crystal lattice. The critical properties of the magnetic specific heat are therefore difficult to measure in a standard specific heat capacity setup. Here the birefringence is an elegant way to determine the critical exponent  $\alpha$  as well as the amplitude ratio  $A^+/A^-$  of the critical part of the specific heat capacity above and below the phase transition.

## III. RESULTS

Figure 3 shows the temperature dependence of  $n_{ac}$  over a broad temperature range. At high temperatures,  $n_{ac}$  linearly decreases with lowering temperature. Below about  $T=70$  K there is distinct deviation from linear behavior due to the onset of short ranged 1D correlations along the Ni-chains<sup>9</sup>. The inset in Fig. 3 shows the temperature range of the 3D phase transition in magnification. The onset of 3D correlations close to  $T_N=10.89$  K, which finally leads to a 3D magnetically ordered structure, is indicated by the drop of the birefringence below 11 K.

The derivative of the birefringence with respect to tem-

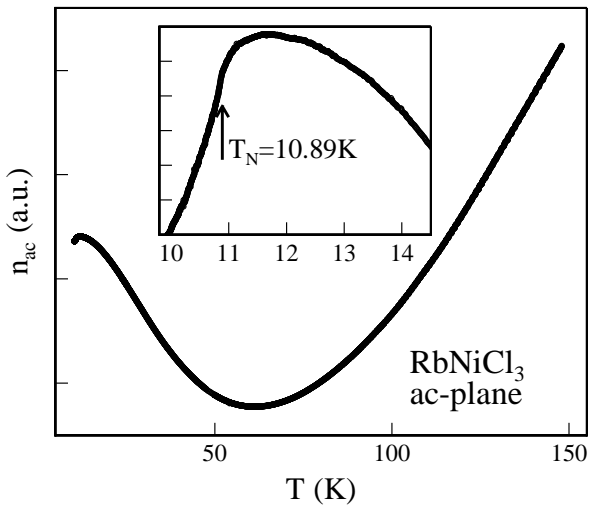


FIG. 3: Temperature dependence of the birefringence  $n_{ac} = n_c - n_a$  over a broad temperature range. The inset shows the range of the phase transition in magnification. The transition is marked by an arrow.

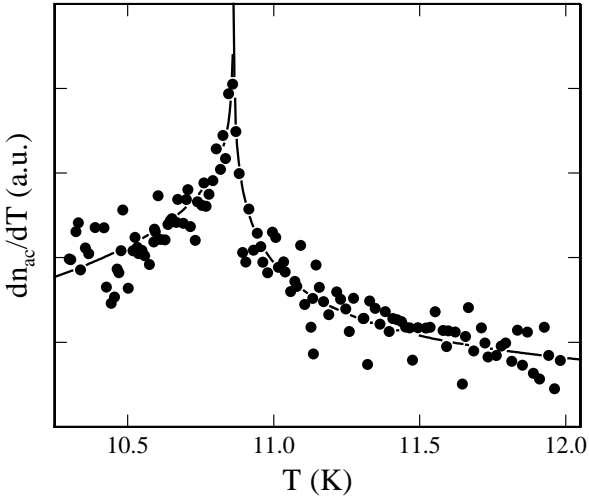


FIG. 4: Temperature-derivative of the critical part of the birefringence,  $dn_{ac}/dT$ , which is proportional to the magnetic specific heat. The solid line is the resulting fit with Eq. (2).

perature is described by a power law:

$$\frac{dn_{ac}}{dT} = A^{\pm} \left| \frac{T - T_N}{T_N} \right|^{-\alpha^{\pm}}. \quad (2)$$

Figure 4 shows  $dn_{ac}/dT$ , the solid line is a fit after Eq. (2). The noncritical contribution due to 1D correlations and lattice natural birefringence was taken into account by a polynomial of the form  $a + bT + cT^2 + dT^3 + eT^4$  which was subtracted from the data. We observe only one transition as the fitted transition temperatures for the range below and above  $T_N$  perfectly coincide. The

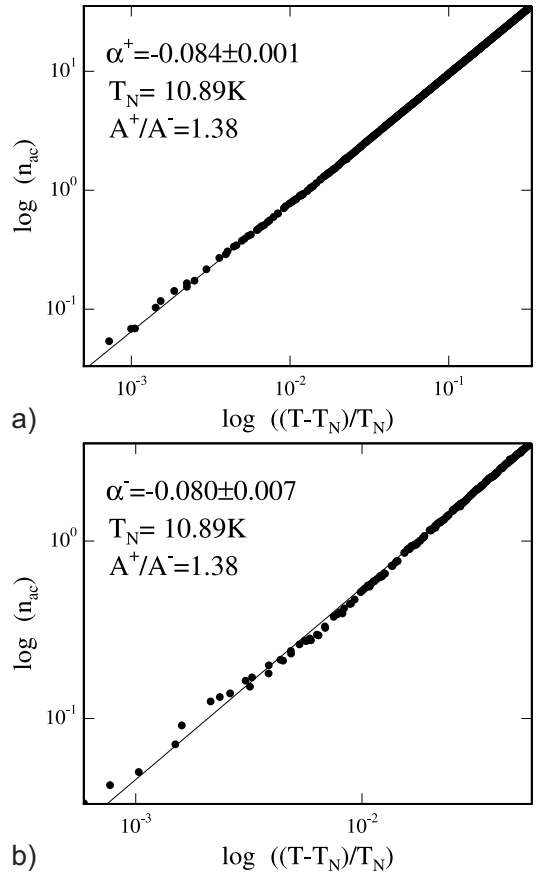


FIG. 5: Log-log plots of the critical part of the birefringence  $n_{ac}$  vs. reduced temperature  $|t| = |(T - T_N)/T_N|$  for (a)  $T > T_N$  and (b)  $T < T_N$ . Solid lines are fits with Eq. (2), the fitted values for  $\alpha^{\pm}$ ,  $T_N$  and the ratio  $A^+/A^-$  are given in the figure.

good temperature resolution allows to measure as close to the phase transition as  $10^{-4}$  in reduced temperature, considerably closer than all previous experiments. Even if two different transition temperatures were allowed for the high and the low temperature side, they converge to a single one in the fit. We do not observe any signs of crossover effects. To check the quality of the fits, Fig. 5 shows log-log plots of the critical part of  $n_{ac}$  vs. reduced temperature  $|t| = |(T - T_N)/T_N|$  for  $T \leq T_N$  in the range close to the phase transition.  $T_N$  is determined to  $T_N = 10.888 \pm 0.001$  K, the values for  $\alpha$  from the high and the low temperature side to  $\alpha^+ = 0.084 \pm 0.001$  and  $\alpha^- = 0.080 \pm 0.007$ . The ratio  $A^+/A^-$  is obtained to  $1.38 \pm 0.07$ . Comparing these values with those from Tab. I, the determined critical exponent and  $A^+/A^-$  agree remarkably well with those of a Heisenberg anti-ferromagnet on the rectangular lattice. Chiral or XY-behavior, as predicted in the chiral theory, can be excluded. Two close lying successive phase transitions that would lead to a rounded anomaly in the measurements can obviously be excluded by our measurements in Figs. 4 and 5.

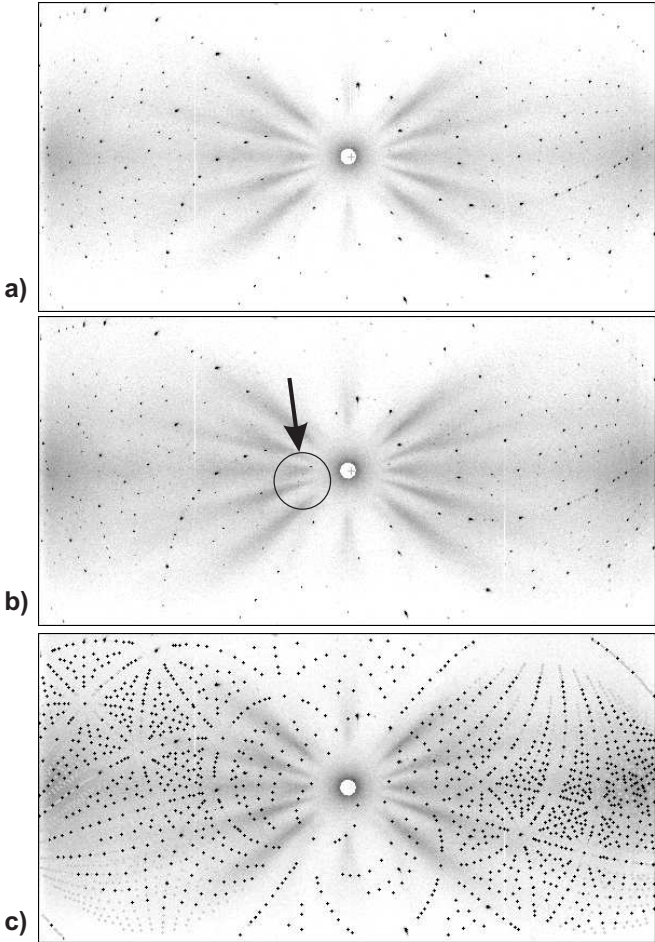


FIG. 6: Laue-photographs taken at different temperatures. (a)  $T=20$  K, above phase transition; (b)  $T=2$  K, in the magnetically ordered phase (some of the magnetic superlattice reflections are marked by the arrow); (c)  $T=2$  K with predicted Laue-pattern.

The unusual behavior of  $\text{RbNiCl}_3$  might be explained by a lift of degeneracy of the magnetic exchange interactions in the hexagonal basal plane. This scenario has been discussed for other  $\text{ABX}_3$  compounds in e.g. [3,22]. Considering the crystal structure of  $\text{RbNiCl}_3$ , as pictured in Fig. 2, a lift of degeneracy is inseparable from changes in the crystal lattice. We therefore carried out supplementary single-crystal neutron diffraction experiments at the new Vivaldi Laue-diffractometer at the high flux reactor of the ILL in Grenoble, France, to detect a possible change in the lattice symmetry below  $T_N$ . Vivaldi's large image plate thereby allows to survey large areas of reciprocal space to detect possible superlattice reflections in the ordered phase. Typical sample crystals of about  $1 \times 1 \times 2$  mm $^3$  were mounted in a helium orange cryostat. We took exposures at  $T=20$  K, in the paramagnetic, and in the ordered phase, at 2 K. The corresponding Laue patterns are shown in Fig. 6. The reflections of the  $T=20$  K exposure in Fig. 6 (a) could be indexed by a primitive hexagonal cell with lattice parameters  $a=6.93$  Å

and  $c=5.89$  Å. The reflections in the magnetically ordered phase can be described in terms of a tripled hexagonal cell ( $a\sqrt{3}, a\sqrt{3}, c$ ). We could not detect any splitting of the reflections below the phase transition within the experimental angular resolution of  $10'$  nor the appearance of additional superlattice reflections which are not indexed by the tripled hexagonal cell. Our measurements therefore confirm the previous results by Yelon and Cox<sup>7</sup>.

#### IV. DISCUSSION

The question arises, why  $\text{RbNiCl}_3$  - which belongs to the same material class as  $\text{CsNiCl}_3$  - does not show two successive phase transitions and the predicted chiral critical behavior. Two successive phase transitions can be excluded from our high resolution birefringence measurements as well as from most of the previously reported experimental results. Close lying divergences due to two close lying phase transition should lead to a rounded anomaly in the measurements. But even in the high resolved data of Fig. 4, the anomaly remains sharp and pronounced confirming the single phase transition observed in a previous LMB study<sup>10</sup> and other techniques (see the listing in Tab II). The Heisenberg critical exponent  $\alpha$  and the ratio  $A^+/A^-$  correspond to conventional critical behavior and therefore point to a, at least partial, lift of frustration below  $T_N$ . A lattice distortion in the ordered phase can be excluded by the neutron diffraction data. If there was only one transition, connected with ordering of the spin components parallel and perpendicular to the 1D axis but no ordering of the chirality, the corresponding transition should indeed show conventional Heisenberg critical behavior for antiferromagnets on rectangular lattices. We therefore argue that spin fluctuations suppress long ranged chiral order in  $\text{RbNiCl}_3$  below  $T_N$ .

The chirality, which basically takes into account the sense of rotation of the spin direction on a chosen triangle, is defined as<sup>23</sup>:

$$\vec{\kappa} = \frac{2}{3\sqrt{3}} (\mathbf{S}_i \times \mathbf{S}_j + \mathbf{S}_j \times \mathbf{S}_k + \mathbf{S}_k \times \mathbf{S}_i). \quad (3)$$

Figure 7 shows the ordered spin structure of  $\text{RbNiCl}_3$  in the hexagonal basal plane, as proposed in the literature. The spins lie in a [001][110] plane with  $2/3$  of the spins canted away from  $c$  by an angle  $\theta$ .  $\theta$  depends on the ratio  $D/J'$  and is determined to  $\theta=57.5$  °<sup>7</sup> in  $\text{RbNiCl}_3$ , very close to the ideal value of  $60$  °. In this model, the chirality  $\vec{\kappa}$  is long ranged ordered and changes sign from one to the neighboring triangle, respectively. Oohara and Iio investigated the  $\text{RbNi}_{1-x}\text{Co}_x\text{Cl}_3$  system<sup>14</sup> with LMB. By replacing  $\text{Ni}^{2+}$  by  $\text{Co}^{2+}$ , the magnitude of the Ising anisotropy  $D$ , which is very small in pure  $\text{RbNiCl}_3$  (70 % that of  $\text{CsNiCl}_3$ ), can gradually be increased. With increasing  $D$ , two anomalies become visible in the LMB experiments and the distance  $T_{N1}-T_{N2}$  increases. The latter study clearly shows that the small Ising anisotropy

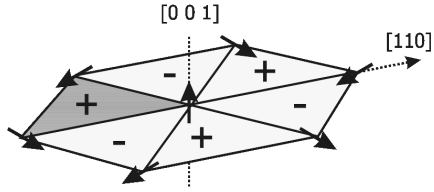


FIG. 7: In the magnetically ordered phase of  $\text{RbNiCl}_3$  as proposed in literature,  $2/3$  of the spins are canted away from  $c$  in the  $[110]$  direction. The chirality  $\vec{\kappa}$  changes sign from one triangle to the neighboring triangle.

$D$  plays the crucial role for the understanding of criticality and phase transitions in  $\text{RbNiCl}_3$ . It also proves that LMB is capable to detect the upper transition, if any.

The anisotropy  $D$  confines the  $120^\circ$  spin structure in the  $ac$  plane. Depending on the ratio  $D/J'$ , the structure might exhibit an additional degree of freedom connected with the rotation of the  $120^\circ$  structure in the  $ac$  plane. This *quasidegeneracy* has been predicted<sup>24</sup> and experimental evidence was found for the case of  $\text{CsNiCl}_3$ <sup>25</sup>. The energy barrier for a rotation of the spin-star in the  $ac$  plane is of the order of  $D(D/6J')^{211}$ . Miyashita<sup>24</sup> suggested, that the this quasidegeneracy exists, if  $(D/J') < 1$  ( $D/J' = 0.06$  in  $\text{RbNiCl}_3$ ). Even though  $D_{\text{RbNiCl}_3} = 0.7D_{\text{CsNiCl}_3}$ ,  $D(D/6J')^2$  for  $\text{RbNiCl}_3$  is just 7 % of that of  $\text{CsNiCl}_3$ ; the quasidegeneracy should therefore be strongly enhanced in the paramagnetic phase of pure  $\text{RbNiCl}_3$ .

NMR and measurements of the specific heat capacity (see Tab. II) give evidence for strong spin fluctuations also in the ordered phase of  $\text{RbNiCl}_3$ . Figure 8 schematically shows the two basic spin relaxation mechanisms. Type I fluctuations are rotations of the spin-star around an axis perpendicular to the spin plane, i.e. parallel to the chirality vector  $\vec{\kappa}$ . This is the quasidegeneracy that has been discussed above. As indicated in the figure, these fluctuations preserve the chirality of the triangle;  $\vec{\kappa}$  can still show long ranged order. All fluctuations with axis of rotation perpendicular to  $\vec{\kappa}$  (Type II fluctuations) change the sign of  $\vec{\kappa}$ . In this case, as long as the fluctuations are not completely coherent (what is quite unlikely), no order of  $\vec{\kappa}$  can be expected and the phase transition should be of conventional type, as suggested by the LMB experiment. Some qualitative comments are in order: Type II fluctuations seem to be at no cost against the Ising anisotropy  $D$  because the canting angle of the respective spins does not change during the rotation. But they are likely to be energetically less favorable than Type I fluctuations, because the spin-star has to be turned out of the canting plane of the spins. The probability of Type II fluctuations seems to scale, however, with the probability of Type I fluctuations because they play a major role when Type I fluctuations are strongly enhanced (as in pure  $\text{RbNiCl}_3$ ), only. In  $\text{CsNiCl}_3$ , or when the Ising anisotropy is enlarged in the  $\text{RbNi}_{1-x}\text{Co}_x\text{Cl}$  system, the contribution of Type II fluctuations is obviously negligible as these compounds show ordering as predicted by

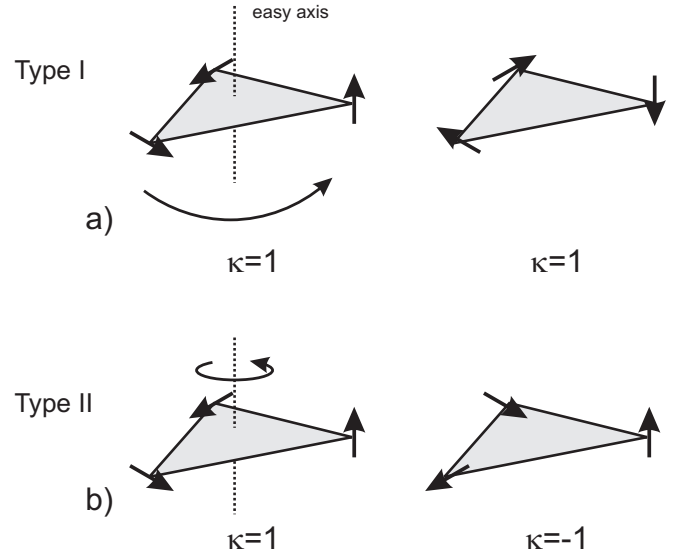


FIG. 8: Fluctuations of the triangle marked in Fig. 7: (a) Type I: Rotations about an axis parallel to the vector of chirality  $\vec{\kappa}$  preserve the chirality. (b) Type II: Fluctuations around the easy-axis, perpendicular to  $\vec{\kappa}$ , change sign of the chirality.

theory.

Nevertheless does the picture of fluctuations which on the one hand preserve (Type I) and on the other hand suppress (Type II) long ranged chiral order account well for phase transitions and critical behavior observed in  $\text{RbNiCl}_3$ . The upper transition at  $T_{N1}$ , connected with ordering of the spin components parallel to the 1D axis, is presumably suppressed by Type I fluctuations; Type II fluctuations do not change the projection of the magnetic moment onto the  $c$ -axis. But fluctuations of Type II might suppress ordering of the chirality  $\vec{\kappa}$  at the lower transition  $T_{N2}$  (whereas Type I fluctuations have no effect on the sign of  $\vec{\kappa}$ ). If both types of fluctuations are strongly enhanced, there should be just one phase transition, connected with ordering of the parallel and perpendicular component and no long ranged ordered chirality. The corresponding critical exponents should show conventional critical behavior for antiferromagnets on rectangular lattices, as it is observed in the LMB experiment. We argue that the very small Ising anisotropy  $D$  leads to a pronounced Heisenberg character of  $\text{RbNiCl}_3$ . Enhanced spin fluctuations of the above mentioned types yield to a different phase diagram and different critical behavior, as compared to other members of the  $\text{ABX}_3$  family.

## V. CONCLUSIONS

We present a linear magnetic birefringence study in  $\text{RbNiCl}_3$ . Our high resolution determination of the critical parameters  $\alpha$  and the amplitude ratio  $A^+/A^-$  show conventional Heisenberg critical behavior for antiferromagnets on rectangular lattices as opposed to theoreti-

ical predictions. There is just one phase transition in  $\text{RbNiCl}_3$ . From a neutron diffraction study we can exclude a structural phase transition and a lift of the degeneracy of the magnetic exchange interactions in the basal plane at  $T_N$ . We discuss  $\text{RbNiCl}_3$  in the framework of previous experimental and theoretical results and other members of the  $\text{ABX}_3$  family. Supported by results in the literature, we finally argue that spin fluctuations lead to the unusual behavior of  $\text{RbNiCl}_3$ . The first phase transition at  $T_{N1}$ , connected with ordering of the spin component parallel to the easy-axis might be suppressed by spin fluctuations with axis of rotation parallel to the chirality vector  $\vec{\kappa}$  (Type I fluctuations). Fluctuations of Type II, with axis of rotation perpendicular to  $\vec{\kappa}$ , presumably suppress long ranged order of the chirality  $\vec{\kappa}$  and lead to a

lift of frustration at  $T_N$ . The resulting single phase transition then shows conventional critical behavior, thereby explaining the critical exponents and phase transitions observed in the LMB experiment.

### Acknowledgments

We are indebted to and thank K. Knorr for hospitality and fruitful discussions. This work has been partially funded by the Universität des Saarlandes, Saarbrücken, Germany. We thank H. Tanaka for providing us with the high quality samples.

---

\* Present address: Institut Laue-Langevin, 6 rue Jules Horowitz, BP 156, 38042 Grenoble Cedex 9, France; Electronic address: rheinstaedter@ill.fr

<sup>1</sup> H. Kawamura, *J. Appl. Phys.* **61**, 3590 (1987).

<sup>2</sup> M. Tissier, B. Delamotte, and D. Mouhanna, *Phys. Rev. Lett.* **84**, 5208 (2000).

<sup>3</sup> M. Collins and O. Petrenko, *Can. J. Phys.* **75**, 605 (1997).

<sup>4</sup> H. Kawamura, *Phys. Soc. Jpn.* **61**, 1299 (1992).

<sup>5</sup> H. Kawamura, *Phys. Rev. B* **47**, 3415 (1993).

<sup>6</sup> K. Nakajima, K. Kakurai, H. Hiraka, H. Tanaka, K. Iio, and Y. Endoh, *J. Phys. Soc. Jpn.* **61**, 3355 (1992).

<sup>7</sup> W. Yelon and D. Cox, *Phys. Rev. B* **6**, 204 (1972).

<sup>8</sup> Y. Oohara, H. Kadokawa, and K. Iio, *J. Phys. Soc. Jpn.* **60**, 393 (1991).

<sup>9</sup> K. Iio, H. Hyodo, and K. Nagata, *J. Phys. Soc. Jpn.* **49**, 1336 (1980).

<sup>10</sup> Y. Oohara, K. Iio, H. Tanaka, and K. Nagata, *J. Phys. Soc. Jpn.* **60**, 4280 (1991).

<sup>11</sup> Y. Oohara and K. Iio, *J. Phys. Soc. Jpn.* **63**, 4597 (1994).

<sup>12</sup> S. Muneta, S. Maegawa, A. Oyamada, T. Goto, and Y. Oohara, *J. Magn. Magn. Mater.* **140-144**, 1787 (1995).

<sup>13</sup> H. Tanaka, K. Nagata, and K. Iio, *J. Magn. Magn. Mater.* **104**, 829 (1992).

<sup>14</sup> H. Tanaka, T. Hasegawa, and K. Nagata, *J. Phys. Soc. Jpn.* **62**, 4053 (1993).

<sup>15</sup> P. Johnson, J. Rayne, and S. Friedberg, *J. Appl. Phys.* **50**, 1853 (1979).

<sup>16</sup> J. Rayne, J. Collins, and G. White, *J. Appl. Phys.* **52**, 1977 (1981).

<sup>17</sup> S. Collocot and J. Rayne, *J. Appl. Phys.* **61**, 4404 (1987).

<sup>18</sup> D. Beckmann, J. Wosnitza, and H. v. Löhneysen, *Phys. Rev. Lett.* **71**, 2829 (1983).

<sup>19</sup> H. Senarmont, *Ann. Chim. Phys.* **73**, 337 (1840).

<sup>20</sup> D. Belanger, A. King, and V. Jaccarino, *Phys. Rev. B* **29**, 2636 (1984).

<sup>21</sup> J. Ferré and G. Gehring, *Rep. Prog. Phys.* **47**, 513 (1984).

<sup>22</sup> M. Zhitomirsky, O. Petrenko, and L. Prozorova, *Phys. Rev. B* **52**, 3511 (1995).

<sup>23</sup> H. Kawamura, *J. Appl. Phys.* **63**, 3086 (1988).

<sup>24</sup> S. Miyashita, *J. Phys. Soc. Jpn.* **55**, 3605 (1986).

<sup>25</sup> S. Maegawa, T. Goto, and Y. Ajiro, *J. Phys. Soc. Jpn.* **57**, 1402 (1988).